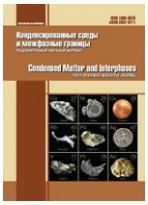

ISSN 1606-867X (Print)
ISSN 2687-0711 (Online)
Condensed Matter and Interphases
Kondensirovannye Sredy i Mezhfaznye Granitsy
https://journals.vsu.ru/kcmf/

Original articles

Research article
https://doi.org/10.17308/kcmf.2025.27/13298

Experimental study of phase equilibria in the Cu_2SnSe_3-Cu_3SbSe_4-Se ternary system

E. N. Ismayilova[1]✉, L. F. Mashadiyeva[1], I. B. Bakhtiyarly[1], V. A. Gasymov[1], I. F. Huseynova[1], Y. I. Jafarov[2]

[1]Institute of Catalysis and Inorganic Chemistry n.a. M. Nagiyev, 113 H. Javid av., Baku Az1143, Azerbaijan

[2]Baku State University, 33 Zahida Khalilova av., Baku Az1148, Azerbaijan

Abstract

Objectives: Copper-tin and copper-antimony chalcogenides are highly desirable for the creation of novel, affordable, and ecologically friendly thermoelectric materials. Due to the potential for improving their thermoelectric performance through different cationic and anionic substitutions, these compounds have recently attracted increased attention. The aim of the work was to establish the nature of the physicochemical interaction in the Cu_2SnSe_3-Cu_3SbSe_4-Se compositions region of the Cu-Sn-Sb-Se quaternary system by experimentally studying phase equilibria.

Experimental: Elemental components of high purity (⩾ 99.999 %) from EVOCHEM Advanced Materials GmbH (Germany) were used for the synthesis of the ternary compounds. The synthesis was carried out in evacuated (~10^{-2} Pa) quartz ampoules at temperatures 50 °C above the melting points of the ternary compounds. Phase equilibria in the Cu_2SnSe_3*Cu_3SbSe_4-Se system were experimentally studied using differential thermal analysis (NETZSCH 404 F1 Pegasus system) and X-ray diffraction (diffractometer Bruker D2 PHASER). This paper presents the *T-x* diagram of the Cu_2SnSe_3-Cu_3SbSe_4 boundary system, the isothermal section at 300 K, the liquidus surface projection, as well as three polythermal sections of the phase diagram. The primary crystallization fields of the phases and the types and coordinates of non- and monovariant equilibria are also determined.

Conclusions: The Cu_2SnSe_3-Cu_3SbSe_4 system has been established to be a quasi-binary eutectic system. Eutectic equilibrium is established at 68 mol % Cu_3SbSe_4 and 727 K. The liquidus surface of the studied system consists of two wide regions of primary crystallization of the Cu_2SnSe_3 and Cu_3SbSe_4 phases and one degenerate region near the selenium corner of the concentration triangle. A wide immiscibility area of two liquid phases is observed in the system, which has the form of a continuous solid solutions between the corresponding regions of the Cu_2SnSe_3-Se and Cu_3SbSe_4-Se boundary systems.

Keywords: Copper-antimony-tin selenides, Phase diagram, Immiscibility region, Solid solutions

For citation: Ismayilova E. N., Mashadiyeva L. F., Bakhtiyarly I. B., Gasymov V. A., Huseynova I. F., Jafarov Y. I. Experimental study of phase equilibria in the Cu_2SnSe_3-Cu_3SbSe_4-Se ternary system. *Condensed Matter and Interphases*. 2025;25(4): 606–614. https://doi.org/10.17308/kcmf.2025.27/13298

Для цитирования: Исмаилова Э. Н., Машадиева Л. Ф., Бахтиярлы И. Б., Гасымов В. А. Гусеинова И. Ф., Джафаров И. Я. Экспериментальное исследование фазовых равновесий в тройной системе Cu_2SnSe_3-Cu_3SbSe_4-Se. *Конденсированные среды и межфазные границы*. 2025;25(4): 606–614. https://doi.org/10.17308/kcmf.2025.27/13298

✉ Elnara N. Ismayilova, e-mail: eismayilova672@gmail.com

Introduction

During the global energy and climate crisis, the widespread use of thermoelectric (TE) materials in low-emission energy conversion technologies is a key priority in the scientific community [1–5]. Among these materials, multicomponent chalcogenides, especially those based on Cu, have attracted considerable attention as environmentally friendly materials [6–13]. Many of these compounds, due to their optical and electronic properties, can be used in various types of electrical devices such as electrochemical sensors, solid-state electrolytes, ion-selective electrodes, displays, etc. In particular, phases of variable composition formed in Cu-Sn-Sb-X systems and being synthetic analogs of the tetrahedrite mineral $Cu_{12}Sb_4S_{13}$ exhibit high ZT values and can be considered good candidates as thermoelectric materials [14–20]. It is well known that changing the composition and structure of materials is one of the effective methods for optimizing their functional properties. On the other hand, the availability of reliable data on phase equilibria and thermodynamic properties of the corresponding multicomponent systems is particularly important for the search and development of new materials and a better understanding of the relationship between composition, structure, and properties [21–30]. For this reason, it is advisable to conduct studies of the physicochemical interactions in the Cu–Sn–Sb–Se system, identify the phases of variable composition formed in it, and establish a general picture of phase equilibria.

In our earlier reports, phase equilibria in the Cu-Sn-Sb-Se system were studied in the composition ranges of Cu_2Se-Cu_2SnSe_3-Cu_3SbSe_4, Cu_2Se-$SnSe$-Sb_2Se_3, and Cu_2SnSe_3-Sb_2Se_3-Se using differential thermal analysis (DTA) and X-ray diffraction (XRD) [31-34]. The fields of primary crystallization of phases and the boundaries of homogeneity regions were determined, and the characters and types of non- and monovariant equilibria of these systems were established. It was found that the quaternary compound $CuSnSbSe_3$ is formed by a peritectic reaction in the Cu_2Se-$SnSe$-Sb_2Se_3 system and exists in a very narrow temperature range (~ 650–723 K) [33].

In this paper, we present the results of a study of phase equilibria in the Cu_2SnSe_3-Cu_3SbSe_4-Se system over the entire concentration range. This region plays an important role in determining the complete picture of phase equilibria in the Cu_2Se-$SnSe_2$-Sb_2Se_3-Se system. The ternary compound Cu_2SnSe_3 melts with an open maximum at 968 K and undergoes a polymorphic transition at 948 K [35, 36]. The high-temperature cubic phase of this compound has a lattice parameter a = 5.6877 Å [35, 37]. Below the polymorphic transition point, the monoclinic phase (Sp. Gr.*Cc*) crystallizes with the following unit cell parameters: a = 6.9670±3 Å, b = 12.0493 ± 7 Å, c = 6.9453 ± 3 Å, β = 109.19(1)°; z = 4 [38, 39]. The compound Cu_3SbSe_4 melts congruently at 755 K and has a tetragonal crystal structure (Sp. Gr. *I*42*m*) with the lattice parameters: $a = b$ = 5.6609 (8) Å; c = 11.280 (5) Å [40].

Both boundary side Cu_2SnSe_3-Se and Cu_3SbSe_4-Se of the studied Cu_2SnSe_3-Cu_3SbSe_4-Se quasi-ternary system are quasi-binary. The Cu_2SnSe_3-Se system is characterized by presence of the monotectic and eutectic equilibria [36]. At the monotectic temperature (910 K), the region of immiscibility of the two liquid phases covers the composition range of 37–95 at. % elemental Se (these numbers refer to the scale of $1/6Cu_2SnSe_3$-Se, i.e., 1 g-atomic amounts of the compound and elemental selenium). The eutectic point is degenerate near the selenium corner of the concentration triangle. The character of the phase equilibria of the $1/8Cu_3SbSe_4$-Se system is qualitatively identical to the previous $1/6Cu_2SnSe_3$-Se system. At the monotectic temperature, the immiscibility region extends over a wide composition range of ~ 10–97 at. % Se, and the eutectic is also degenerate near Se [36]. In [41], the formation of solid solutions with Sn-Sb substitution in the Cu_2SnSe_3-Cu_3SbSe_4 system at 673 K was established, and their thermoelectric properties were studied. However, there is no information in the literature on the phase diagram of this system.

2. Experimental

2.1. Synthesis

High-purity (⩾ 99.999 %) primary components from EVOCHEM Advanced Materials GmbH (Germany) were used for the synthesis. Ternary compounds of the studied system were obtained by melting simple substances in stoichiometric ratios corresponding to the Cu_2SnSe_3 and

Cu_3SbSe_4 formulas. The synthesis was carried out in evacuated (~10^{-2} Pa) quartz ampoules at temperatures 50 °C above the melting points of the ternary compounds [36]. After synthesis, the furnace was shut off and the ampoules were slowly cooled to room temperature and then annealed at 700 K for 50 hours to obtain a homogeneous stoichiometric composition.

The individuality of the synthesized ternary compounds was controlled using differential thermal analysis (DTA) and powder X-ray diffraction (XRD). The determined melting point and crystal lattice parameters for the two synthesized compounds were similar to the literature data given above within the margin of error (± 3 K and ± 0.0003 Å) [35–40].

To conduct the experiments, 32 samples were prepared along the 1/6Cu_2SnSe_3-[B], [A]-1/8 Cu_3SbSe_4, and [C]-Se cross-sections, as well as some additional alloys outside these cross-sections, by melting the initial compounds in a vacuum. According to the DTA of cast non-homogenized samples, their crystallization from melts is complete at 500 K. Therefore, to achieve a state as close to equilibrium as possible, the obtained cast alloys were annealed at 450 K for 400 h.

2.2. Research methods

DTA and XRD were used for the studies. Equilibrium samples were heated in evacuated quartz ampoules using a NETZSCH 404 F1 Pegasus system differential scanning calorimeter at a heating rate of 10 °C/min. The results were processed using NETZSCH Proteus software. The temperature measurement accuracy was ± 2 K.

X-ray diffraction patterns of the annealed homogenized alloys were obtained at room temperature using a Bruker D2 PHASER diffractometer with CuKα1 radiation. Topaz V3.0 software, provided by Bruker, was used to index the powder diffraction patterns of the studied alloys.

3. Results and discussion

A combination of the DTA and XRD data for three internal sections of the studied system, along with literature data on phase equilibria in boundary quasi-binary systems [34, 39], allowed us to determine the phase equilibria in the Cu_2SnSe_3-Cu_3SbSe_4-Se system. The phase diagram of the Cu_2SnSe_3-Cu_3SbSe_4 boundary system, the solid-phase equilibria diagram of the system at 300 K, the liquidus surface projection, and three polythermal sections of the phase diagram are presented below.

3.1. The Cu_2SnSe_3-Cu_3SbSe_4 quasi-binary section

Powder diffraction patterns of selected intermediate alloys of the studied Cu_2SnSe_3-Cu_3SbSe_4 system are shown in Fig. 1. As can

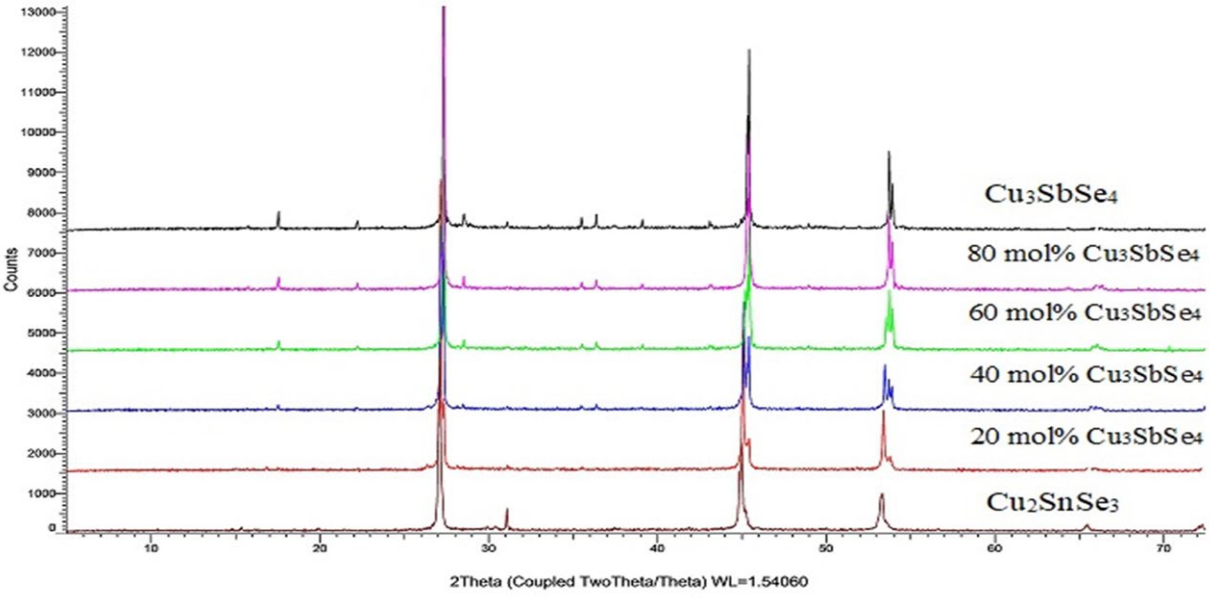

Fig. 1. Powder XRD patterns of alloys of the Cu_2SnSe_3-Cu_3SbSe_4 system

be seen, the diffraction patterns of alloys with compositions of 20 and 80 mol % Cu_3SbSe_4 are qualitatively identical to the diffraction patterns of the initial Cu_2SnSe_3 and Cu_3SbSe_4 compounds, respectively. This indicates the existence of wide solubility regions based on these compounds. Alloys with compositions of 40 and 60 mol % Cu_3SbSe_4 consist of a two-phase mixture of Cu_2SnSe_3+Cu_3SbSe_4 compounds.

Based on DTA and XRD data, a phase diagram of the Cu_2SnSe_3-Cu_3SbSe_4 system was constructed (Fig. 2). It was established that this system is quasi-binary, forms a eutectic-type *T-x* diagram, and is characterized by the formation of wide solid solutions (α- and β-phases) based on both initial components. The liquidus of the system consists of the primary crystallization curves of the α- and β solid solutions. At room temperature, the solubility of Cu_2SnSe_3 and Cu_3SbSe_4 reaches ~30 and ~25 mol %, respectively. The eutectic equilibrium point corresponds to 68 mol % Cu_3SbSe_4 and 727 K. Below the solidus, co-crystallization of the α- and β-phases occurs.

3.2. Isothermal Section at 300 K

According to the solid-phase equilibria diagram (Fig. 3), the Cu_2SnSe_3-Cu_3SbSe_4-Se system consists of two two-phase regions (α + Se and β + Se) and a three-phase region (α + β + Se) separating them.

XRD data of alloys from various regions confirmed their phase composition. As can be seen from Fig. 4, the powder diffractograms of alloys No. 1 and No. 2, shown in Fig. 3, are the sum of the diffraction patterns of the Cu_2SnSe_3 + Se and Cu_3SbSe_4+Se phases, respectively, while the XRD pattern of sample No. 3 contains a set of diffraction lines corresponding to a mixture of α + β + Se.

3.3. Liquidus surface projection (Fig. 5)

The liquidus surface of the studied quasi-ternary system consists of two wide fields of primary crystallization of the α- and β-phases. The immiscibility region that forms on the boundary Cu_2SnSe_3-Se and Cu_3SbSe_4-Se systems penetrates the concentration triangle and forms a wide region of immiscibility of the two liquid phases (L_1 +L_2). The eutectic curve emanating from e_1, corresponding to the eutectic equilibrium of the boundary Cu_2SnSe_3-Cu_3SbSe_4 system, intersects this immiscibility region. As a result, the monovariant eutectic equilibrium $Le_1 \leftrightarrow \alpha+\beta$ is transformed into the nonvariant monotectic equilibrium $L_1 \leftrightarrow L_2 + \alpha + \beta$ (T = 710 K). The compositions of the liquid phases in this equilibrium correspond to points M_1 and M_2. Another nonvariant equilibrium in the system degenerates near the corner of the elementary Se of the concentration triangle. This part of the phase diagram is shown in Fig. 5 at an enlarged scale. At point E, which corresponds to the composition of the ternary eutectic mixture, a

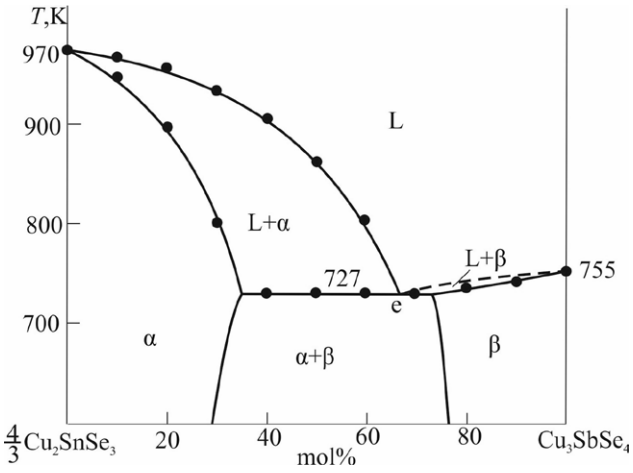

Fig. 2. Phase diagram of the Cu_2SnSe_3-Cu_3SbSe_4 system

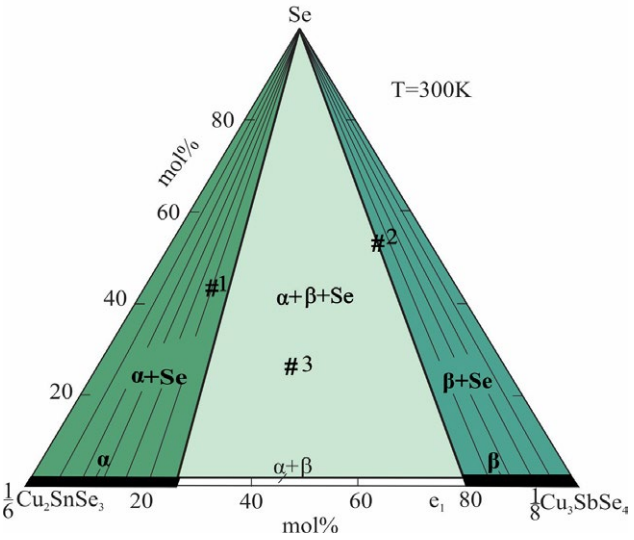

Fig. 3. Solid-phase equilibria diagram of the Cu_2SnSe_3-Cu_3SbSe_4-Se system at 300 K. The composition of the mentioned phases is shown in Fig. 4

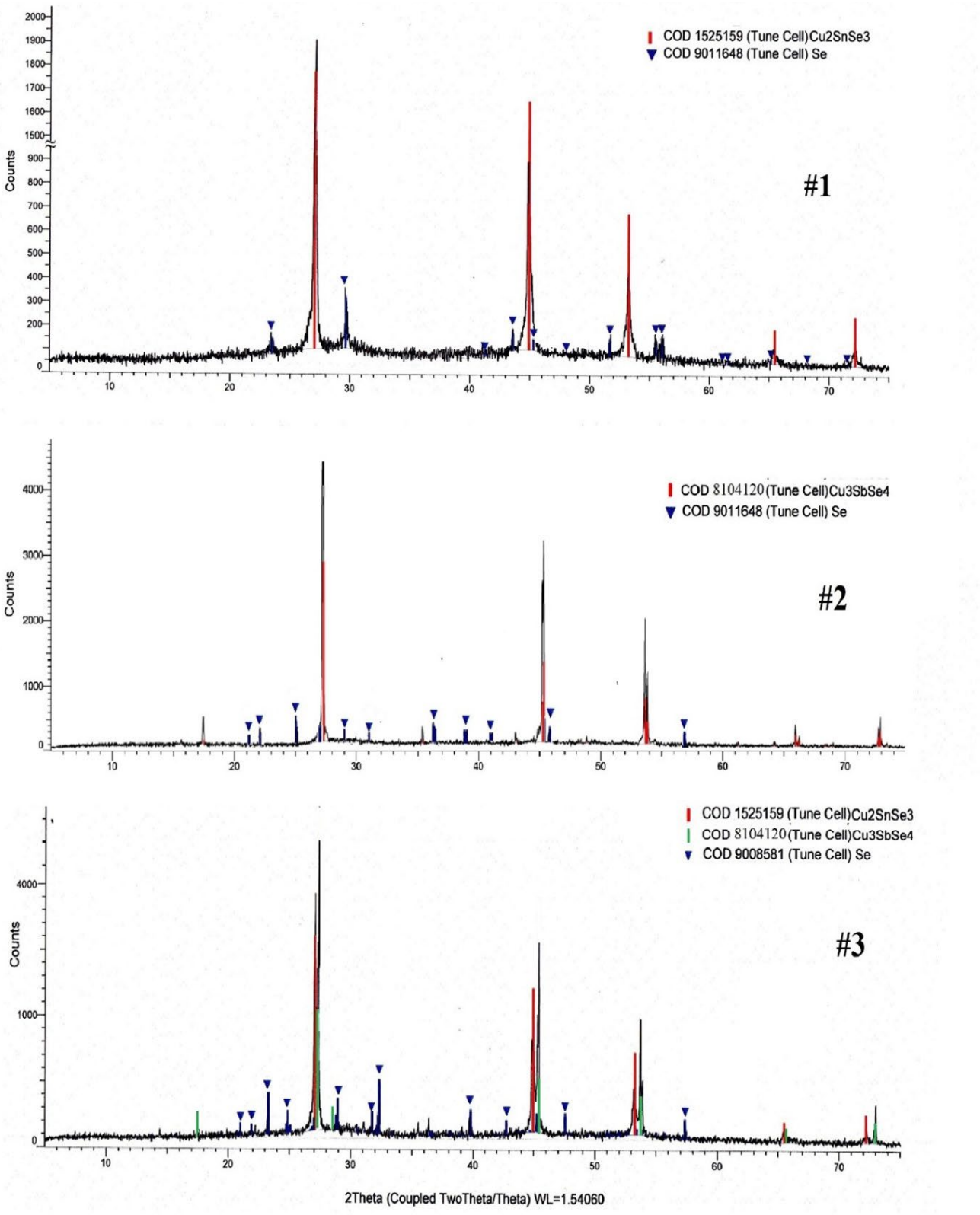

Fig. 4. X-ray powder diffraction patterns of the alloys #1 (50 % Cu_2SnSe_3-50 % Se), #2 (45 % Cu_3SnSe_4-55 % Se), and #3 (40 % Cu_2SnSe_3-30 % Cu_3SnSe_4-30 % Se) in Fig. 3

four-phase eutectic equilibrium L ↔ α + β + Se occurs at 490 K. The conjugate curves (e_2E and e_3E) at the eutectic point (E) degenerate into the following equilibria:

$Le_{2E} \leftrightarrow \alpha + Se$

$Le_{3E} \leftrightarrow \beta + Se$

The immiscibility regions are bounded by the conjugate curves m_1M; $m_1'M'$ и m_2M; $m_2'M'$, which reflect the monovariant monotectic equilibria $L_1 \leftrightarrow L_2 + \alpha$ and $L_1 \leftrightarrow L_2 + \beta$, respectively. The curves e_1M and M'E reflect monovariant eutectic equilibria $L_1 \leftrightarrow \alpha + \beta$ and $L_2 \leftrightarrow \alpha + \beta$ (Fig. 5).

3.4. Polythermal Sections

Polythermal sections of the *T-x-y* phase diagram are important for visualizing crystallization processes in the system.

Section 1/6Cu_2SnSe_3-[B] (Fig. 6). ([B] is an alloy of the 1/8Cu_3SbSe_4-Se side system, corresponding to a 1:1 composition). This region passes through the immiscibility region and the liquidus surface of the α- and β-phases. From left to right, the α-phase crystallizes from the liquid in the range < 55 mol % [B]: L ↔ α. In the 55-85 mol % [B] composition range, the α-phase initially crystallizes from the immiscibility region via the monovariant monotectic reaction $L_1 \leftrightarrow L + \alpha$; and the β-phase crystallizes in the concentration range > 85 mol % [B]. After the primary crystallization of the α-phase based on Cu_2SnSe_3 in the range of ~2–55 mol % [B], crystallization continues via a monotectic reaction. As a result of these processes, the region $L_2 + \alpha$ (L_2 is a liquid based on elemental Se) is formed in Fig. 6. The horizontal line (M) at 710 K in the phase diagram reflects the monovariant equilibrium $L_1 \leftrightarrow L_2 + \alpha + \beta$. This reaction ends with the formation of a three-phase region $L_2 + \alpha + \beta$.

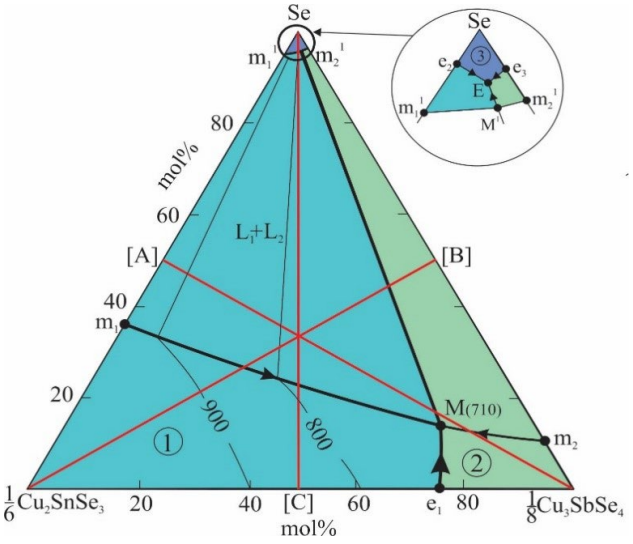

Fig. 5. Liquidus surface of the Cu_2SnSe_3-Cu_3SbSe_4-Se system. Primary crystallization fields: *1* – α (solid solution based on Cu_2SnSe_3); *2* – β (solid solution based on Cu_3SbSe_4); *3* – Se. Red lines are the studied polythermal sections

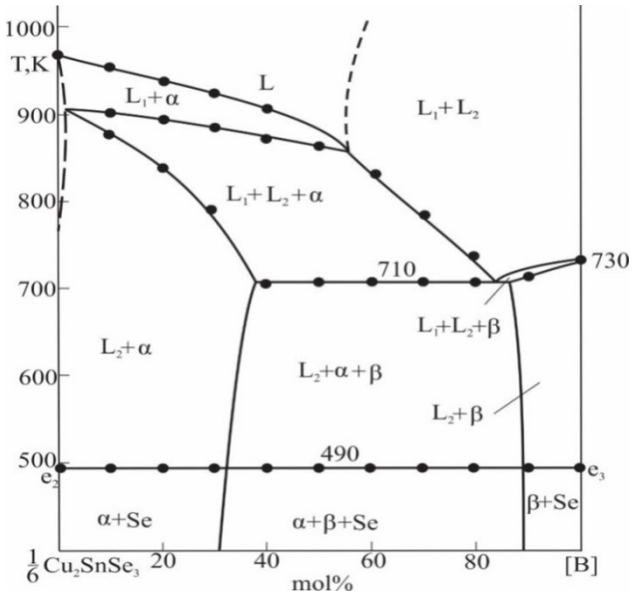

Fig. 6. Polythermal section 1/6Cu_2SnSe_3-[B] system. [B] is alloy of the 1/8 Cu_3SbSe_4-Se boundary system with the composition ratio 1:1

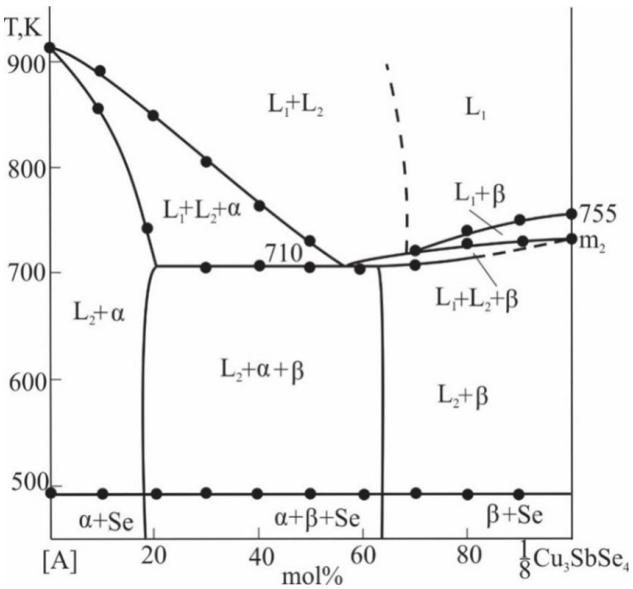

Fig. 7. Polythermal section [A]-1/8Cu_3SbSe_4 system. [A] is an alloy of the 1/6Cu_2SnSe_3-Se boundary system with the composition ratio 1:1

Crystallization is completed by degenerate non- and monovariant eutectic reactions (E, e_2E, e_3E, and M′E) at ~ 490 K, and heterogeneous regions of α + Se, β + Se, and α + β + Se are formed in the subsolidus.

Section [A]-1/8 Cu_3SbSe_4 (Fig. 7). ([A] is an alloy of the $1/6Cu_2SnSe_3$-Se boundary system, corresponding to a 1:1 composition). The crystallization process in this section is somewhat different. Here, the α-phase crystallizes from immiscible liquid phases in the 0–58 mol % 1/8 Cu_3SbSe_4 compositions range. In the ~58–70 mol % 1/8 Cu_3SbSe_4 compositions range, the β-phase initially crystallizes from the L_1+L_2 region, whereas at compositions > 70 mol % 1/8 Cu_3SbSe_4, it crystallizes from the liquid phase L_1. In the composition range of 10-63 mol % 1/8 Cu_3SbSe_4, the system undergoes a nonvariant monotectic equilibrium M, and in the Cu_3SbSe_4-rich region (63–100 mol %), the reaction $L_1 \leftrightarrow L_2$+ β occurs, leading to the formation of the region L_2+ β (Fig. 7).

Thus, the regions L_2+ α, L + α + β, and L_2 + β exist along this section before the crystallization of elemental selenium. As in the previously considered polythermal section, complete crystallization in this section occurs through eutectic reactions, and two-phase mixtures of α + Se, β + Se, and α + β + Se are formed in the solid state.

Section [C]-Se (Fig. 8). (here [C] is an alloy of the boundary system $1/6Cu_2SnSe_3$-$1/8Cu_3SbSe_4$ with a composition of 1:1). This section completely intersects the region of primary crystallization of the α-phase. In the concentration range of ~ 0–23 at. % elemental Se, the α-phase primarily crystallizes from liquid L_1, and in the range of > 95 at. % Se (el.), from liquid L_2. In intermediate compositions, the primary crystallization of the α-phase proceeds according to the monovariant eutectic reaction $L_1 \leftrightarrow L_2$ + α in the L_1 + L_2 immiscibility region. It should be noted that the initial temperature of this process is constant (790 K), indicating that the direction of the L_1-L_2 tie line in the immiscibility region coincides with the plane of this region. Below the liquidus, in the concentration range of 0–10 at. % Se (el.), crystallization continues via the monovariant eutectic reaction $L_1 \leftrightarrow$ α + β, and at 710 K, the system undergoes a four-phase transition reaction: L_1+ α ↔ L_2+ β. Crystallization is completed via the invariant eutectic process L ↔ α + β + Se.

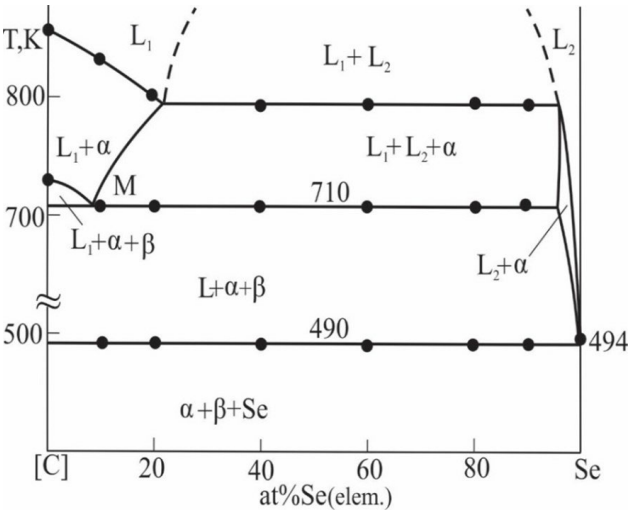

Fig. 8. Polythermal section [C]-Se system. [C] is an alloy of the $1/6Cu_2SnSe_3$-$1/8Cu_3SbSe_4$ boundary system with the composition ratio 1:1

These research results provide the scientific basis for the synthesis and growth of single crystals of selenium-enriched solid solutions based on Cu_2SnSe_3 and Cu_3SbSe_4 compounds.

4. Conclusion

Thus, this study presents a complete picture of phase equilibria in the Cu_2SnSe_3-Cu_3SbSe_4-Se system based on experimental results obtained by differential thermal analysis and X-ray diffraction. It was established that it is a quasi-ternary plane corresponding to the quaternary system. A projection of the liquidus surface and a solid-phase equilibria diagram at 300 K are presented, and a series of polythermal sections is constructed. It is established that the liquidus surface of the phase diagram of the studied quasi-ternary system consists of three primary crystallization fields. The crystallization fields of the α- and β-solid solutions based on Cu_2SnSe_3 and Cu_3SbSe_4 are the most extensive. The region of elemental selenium is degenerate in the corresponding corner of the concentration triangle. A wide region of immiscibility of the two liquid phases is observed in the system, which appears as a continuous band between the corresponding regions of the Cu_2SnSe_3-Se and Cu_3SbSe_4-Se boundary systems.

Author contributions

Ismailova E. N. – study concept, carry out the investigation, compounds synthesis, article writing, and results discussion. Mashadeva L. F. – literature analysis, results discussion. Bakhtiyarly I. B. – results discussion, final conclusions. Gasymov V. A. – XRD results discussion. Huseynova I. F. – compounds synthesis. Dzhafarov Ya. I. – literature review, results discussion.

Conflict of interests

The authors declare that they have no known competing financial interests or personal relationships that could have influenced the work reported in this paper.

References

1. Liu W., Hu J., Zhang S., Deng M., Han C.-G., Liu Y. New trends, strategies and opportunities in thermoelectric materials: a perspective. *Materials Today Physics*. 2017;1: 50–60. https://doi.org/10.1016/j.mtphys.2017.06.001

2. He J., Tritt T. M. Advances in thermoelectric materials research: looking back and moving forward. *Science*. 2017; 357(6358). https://doi.org/10.1126/science.aak9997

3. Jia N., Cao J., Tan X. Y., … Suwardi A.Thermoelectric materials and transport physics. *Materials Today Physics*. 2021;21: 100519. https://doi.org/10.1016/j.mtphys.2021.100519

4. Mukherjee M., Srivastava A., Singh A. K. Recent advances in designing thermoelectric materials *Journal of Materials Chemistry C*. 2022;10: 12524–12555. https://doi.org/10.1039/D2TC02448A

5. Du Y., Xu J., Paul B., Eklund P. Flexible thermoelectric materials and devices. *Applied Materials Today*. 2018;12: 366–388. https://doi.org/10.1016/j.apmt.2018.07.004

6. Qiu P., Shi X., Chen L. Cu-based thermoelectric materials. *Energy Storage Materials*. 2016;3: 85-97. https://doi.org/10.1016/j.ensm.2016.01.009

7.Mikuła A., Mars K., Nieroda P., Rutkowski P. Copper chalcogenide-copper tetrahedrite composites – a new concept for stable thermoelectric materials dased on the chalcogenide system. *Materials*. 2021;14(10): 2635. https://doi.org/10.3390/ma14102635

8. Mulla R., Rabinal M. H. K. Copper sulfides: earth-abundant and low-cost thermoelectric materials. *Energy Technology*. 2019;7(7): 1800850. https://doi.org/10.1002/ente.201800850

9. Jaldurgam F. F., Ahmad Z., Touati F., … Altahtamouni T. Enhancement of thermoelectric properties of low-toxic and earth-abundant copper selenide thermoelectric material by microwave annealing. *Journal of Alloys and Compounds*. 2022;904: 1654131. https://doi.org/10.1016/j.jallcom.2022.164131

10. Wei T.-R., Qin Y., Deng T., … Chen L. Copper chalcogenide thermoelectric materials . *Science China Materials*. 2018;62: 8–24. https://doi.org/10.1007/s40843-018-9314-5

11. Alonso-Vante N. Chalcogenide materials for energy conversion. In: *Nanostructure Science and Technology*. Springer International Publishing; 2018. 226p. https://doi.org/10.1007/978-3-319-89612-0

12. Hu H., Ju Y., Yu J., … Li J.-F. Highly stabilized and efficient thermoelectric copper selenide. *Nature Materials*. 2024;23: 527–534. https://doi.org/10.1038/s41563-024-01815-1

13. Sanghoon X. L., Tengfei L. J., Zhang L. Y-H. *Chalcogenide. From 3D to 2D and beyond*. Elsevier; 2019. 398 p.

14. Wei J., Yang L., Ma Z., … Wang X. Review of current high-ZT thermoelectric materials. *Journal of Materials Science*. 2020;55: 12642–12704 . https://doi.org/10.1007/s10853-020-04949-0

15. Chetty R., Balia A., Mallik R. C. Tetrahedrites as thermoelectric materials: an overview. *Journal of Material Chemistry C*. 2015;3: 12364–12378. https://doi.org/10.1039/C5TC02537K

16. Suekun K., Takabatake T. Research update: Cu–S based synthetic minerals as efficient thermoelectric materials at medium temperatures. *APL Materials*. 2016;4:104503. https://doi.org/10.1063/1.4955398

17. Liu Y., Kretinin A. V., Liu X., … Freer R. Thermoelectric performance of tetrahedrite ($Cu_{12}Sb_4S_{13}$) thin films: the influence of the substrate and interlayer. *ACS Applied Electronic Materials*. 2023;6(5): 2900–2908. https://doi.org/10.1021/acsaelm.3c00909

18. Palchoudhury C. S., Ramasamy K., Gupta A. Multinary copper-based chalcogenide nanocrystal systems from the perspective of device applications. *Nanoscale Advances*. 2020;2(8): 3069–3082. https://doi.org/10.1039/d0na00399a

19. Zhang D., Yang J., Bai H., Yubo L. Significant average ZT enhancement in Cu_3SbSe_4-based thermoelectric material via softening p-d hybridization. *Journal of Materials Chemistry A*. 2019;10: 1039–1048. https://doi.org/10.1039/c9ta05115e

20. Studenyak I. P., Pogodin A. I., Studenyak V. I., … Kúš P. Electrical properties of copper- and silver-containing superionic $(Cu_{1-x}Ag_x)_7SiS_5I$ mixed crystals with argyrodite structure. *Solid State Ion*. 2020;345: 115183–115186. https://doi.org/10.1016/j.ssi.2019.115183

21. Bayramova U. R., Babanly K. N., Ahmadov E. I., Mashadiyeva L. F., Babanly M. B. Phase equilibria in the Cu_2S-Cu_8SiS_6-Cu_8GeS_6 system and thermodynamic functions of phase transitions of the $Cu_8Si_{(1-X)}GeXS_6$ argyrodite phases. *Journal of Phase Equilibria and Diffusion*. 2023;44: 509–519. https://doi.org/10.1007/s11669-023-01054-y

22. Babanly M. B., Yusibov Y. A., Imamaliyeva S. Z., Babanly D. M., Alverdiyev I. J. Phase diagrams in the development of the argyrodite family compounds and solid solutions based on them. *Journal of Phase Equilibria and Diffusion*. 2024;45(12): 228-255. https://doi.org/10.1007/s11669-024-01088-w

23. Babanly M. B., Mashadiyeva L. F., Imamaliyeva S. Z., Babanly D. M., Tagiyev D. B., Yusibov Yu. A. Complex copper-based chalcogenides: a review of phase equilibria and thermodynamic properties Russ. *Condensed Matter and Interphases*. 2024;26(4): 579–619. https://doi.org/10.17308/kcmf.2024.26/12367

24. Mammadov F. M., Babanly D. M., Amiraslanov I. R., Tagiev D. B., Babanly M. B. System FeS–Ga_2S_3–In_2S_3. *Russian Journal of Inorganic Chemistry*. 2021;66(10): 1533–1543. https://doi.org/10.1134/S0036023621100090

25. Abdullayeva Sh. S, Bakhtiyarly I. B, Kurbanova R. J, Mukhtarova Z. M. The quasi-binary $Cu_3In_5S_9$-$FeIn_2S_4$ section. *Condensed Matter and Interphases*. 2022;24(2): 182–186. https://doi.org/10.17308/kcmf.2022.24/9257

26. Mammadov S. H., Mammadov A. N., Kurbanova R .C. Quasi-binary section Ag_2SnS_3–$AgSbS_2$. *Russian Journal of Inorganic Chemistry*. 2020;65(2): 217–221. https://doi.org/10.1134/S003602362001012X

27. Mashadiyeva L. F., Babanly D. M., Hasanova Z. T., Usibov Y. A., Babanly M. B. Phase relations in the Cu-As-S system and thermodynamic properties of copper-arsenic sulfides. *Journal of Phase Equilibria and Diffusion*. 2024:45; 567–582. https://doi.org/10.1007/s11669-024-01115-w

28. Abdullaeva Sh. S., Mammadov F. M., Bakhtiyarly I. B. Quasi-binary section $CuInS_2$–$FeIn_2S_4$. *Russian Journal of Inorganic Chemistry*. 2020;65: 100–105. https://doi.org/10.1134/S0036023619110020

29. Orujlu E. N., Aliev Z. S., Babanly M. B. The phase diagram of the MnTe–SnTe–Sb_2Te_3 ternary system and synthesis of the iso- and aliovalent cation-substituted solid solutions. *Calphad*. 2022;76: 102398. https://doi.org/10.1016/j.calphad.2022.102398

30. Mammadov F. M. New version of the phase diagram of the MnTe- Ga_2Te_3 system. *New Materials*, *Compounds and Applications*. 2021;5(2): 116–121. Available at: http://jomardpublishing.com/UploadFiles/Files/journals/NMCA/V5N2/MammadovF.pdf

31. Ismailova E. N., Mashadieva L. F., Bakhtiyarly I. B., Gasymov V. A., Gurbanova R. J., Mammadova F. M. Phase equilibria in the Cu_2Se - Cu_3SbSe_4 - Cu_2SnSe_3 system. *Chemical Problems*. 2025;23(1): 36–46. https://doi.org/10.32737/2221-8688-2025-1-36-46

32. Ismayilova E. N., Mashadieva L. F., Bakhtiyarly I. B, Babanly M. B. Phase equilibria in the Cu_2SnSe_3–Sb_2Se_3–Se system. *Condensed Matter and Interphases*. 2023;25(1): 47-54. https://doi.org/10.17308/kcmf.2023.25/10973

33. Ismailova E. N., Mashadieva L. F.,Bakhtiyarly I. B, Babanly M. B. Phase equilibria in the Cu_2Se–SnSe–Sb_2Se_3 system. *Azerbaijan Chemical Journal*. 2022;1: 73-82. https://doi.org/10.32737/0005-2531-2022-1-73-82

34. Ismayilova E. N., Baladzhayeva A. N., Mashadiyeva L. F. Phase equılıbrıa along the Cu_3SbSe_4-$GeSe_2$ sectıon of the Cu-Ge-Sb-Se system. *New Materials, Compounds and Applications*. 2021;5(1): 52–58. Available at: https://jomardpublishing.com/UploadFiles/Files/journals/NMCA/V5N1/Ismayilova_et_al.pdf

35. Parasyuk O. V., Olekseyuk I. D., Marchuk O. V. The Cu_2Se–HgSe–$SnSe_2$ system. *Journal of Alloys and Compounds*. 1999;287(1-2): 197–205. https://doi.org/10.1016/S0925-8388(99)00047-X

36. Babanly M. B., Yusibov Yu. A., Abishov V. T. *Three-component chalcogenides based on copper and silver**. Baku: BSU Publ.; 1993. 342 p. (In Russ.).

37. Sharma B. B., Ayyar R., Singh H. Stability of the tetrahedral phase in the $A^I_2B^{IV}C^{VI}_3$ group of compounds. *Physica Status Solidi A*. 1977;40(2): 691–697. https://doi.org/10.1002/pssa.2210400237

38. Marcano G., Chalbaud L., Rincón C., Sánchez P. G. Crystal growth and structure of the semiconductor Cu_2SnSe_3. *Materials Letters*. 2002;53(3): 151–154. https://doi.org/10.1016/s0167-577x(01)00466-9

39. Delgado G. E., Mora A. J., Marcano G., Rincon C. Crystal structure refinement of the semiconducting compound Cu_2SnSe_3 from X-ray powder diffraction data. *Materials Research Bulletin*. 2003;38: 1949–1955. https://doi.org/10.1016/j.materresbull.2003.09.017

40. Pfitzner A. Crystal structure of tri-copper tetraselenoantimonate Cu_3SbSe_4. *Zeitschrift für Kristallographie-Crystalline Materials*. 1994;209(8): 685–685. https://doi.org/10.1524/zkri.1994.209.8.685

41. Fan Y., Xie S., Sun J., Tang X., Tan G. Quasi-isostructural alloying of Cu_2SnSe_3–Cu_3SbSe_4 toward higher thermoelectric performance. *ACS Applied Energy Materials*. 2021;4 (6): 6333–6339. https://doi.org/10.1021/acsaem.1c01155

* *Translated by author of the article*

Information about the authors

Elnara N. Ismayilova, postgraduate student, Researcher, Institute of Catalysis and Inorganic Chemistry of the Ministry of Science and Education of Azerbaijan (Baku, Azerbaijan).

https://orcid.org/0000-0002-1327-1753

eismayilova672@gmail.com

Leyla F. Mashadiyeva, PhD in Chemistry, Senior Researcher, Institute of Catalysis and InorganicChemistry of the Ministry of Science and Education of Azerbaijan (Baku, Azerbaijan).

https://orcid.org/0000-0003-2357-6195

leylafm76@gmail.com

Ikhtiyar B. Bakhtiyarly, Dr. Sci. (Chem.), Professor, Head of Laboratory, Institute of Catalysis and Inorganic Chemistry of the Ministry of Science and Education of Azerbaijan (Baku, Azerbaijan).

https://orcid.org/0000-0002-7765-0672

ibbakhtiarli@mail.ru

Vagif A. Gasymov, Cand. Sci. (Chem.), Associate Professor, Institute of Catalysis and Inorganic Chemistry of the Ministry of Science and Education of Azerbaijan (Baku, Azerbaijan).

https://orcid.org/0000-0001-6233-5840

vgasymov@rambler.ru

Ilahe F. Huseynova, PhD in Chemistry, Institute of Catalysis and Inorganic Chemistry of the Ministry of Science and Education of Azerbaijan (Baku, Azerbaijan).

https://orcid.org/0000-0002-1106-0207

mehdiyeva.ilahe2@gmail.com

Yasin Isa Jafarov, Dr. Sci. (Chem.), Associate Professor, Baku State University (Baku, Azerbaijan).

https://orcid.org/0000-0002-3968-8725

yasin_cafarov@mail.ru

Received March 6, 2025; approved after reviewing April 2, 2025; accepted for publication May 15, 2025; published online December 25, 2025.